



Cu(II), Co(II), Ni(II), Mn(II), and Fe(II) metal complexes containing *N,N'*-(3,4-diaminobenzophenon)-3,5-Bu^t₂-salicylaldimine ligand: Synthesis, structural characterization, thermal properties, electrochemistry, and spectroelectrochemistry

E. Tas^{a,*}, A. Kilic^b, M. Durgun^b, L. Küpecik^b, I. Yilmaz^c, S. Arslan^d

^a Department of Chemistry, University of Siirt, 56100 Siirt, Turkey

^b Department of Chemistry, University of Harran, 63190 Sanliurfa, Turkey

^c Department of Chemistry, Technical University of Istanbul, 34469, Istanbul, Turkey

^d Department of Chemistry, University of Nevsehir, 50300 Nevsehir, Turkey

ARTICLE INFO

Article history:

Received 9 February 2009

Received in revised form

20 November 2009

Accepted 1 December 2009

Keywords:

Synthesis

Schiff bases

Metal complexes

Thermal properties

Electrochemistry

Spectroelectrochemistry

ABSTRACT

The synthesis, structure, spectroscopic and electro-spectrochemical properties of steric hindered Schiff-base ligand [*N,N'*-(3,4-benzophenon)-3,5-Bu^t₂-salicylaldimine (LH₂)] and its mononuclear Cu(II), Co(II), Ni(II), Mn(II) and Fe(II) complexes are described in this work. The new dissymmetric steric hindered Schiff-base ligand containing a donor set of NONO was prepared through reaction of 3,4-diaminobenzophenon with 3,5-Bu^t₂-salicylaldehyde. Certain metal complexes of this ligand were synthesized by treating an ethanolic solution of the ligand with an equimolar amount of metal salts. The ligand and its complexes were characterized by FT-IR, UV-vis, ¹H NMR, elemental analysis, molar conductivity and thermal analysis methods in addition to magnetic susceptibility, electrochemistry and spectroelectrochemistry techniques. The tetradentate and mononuclear metal complexes were obtained by reacting *N,N'*-(3,4-benzophenon)-3,5-Bu^t₂-salicylaldimine (LH₂) with some metal acetate in a 1:1 mole ratio. The molar conductance data suggest metal complexes to be non-electrolytes.

© 2009 Elsevier B.V. All rights reserved.

1. Introduction

Tetradentate metal complexes of Schiff bases afford mixed donor environments and an open equatorial ring, the hole size of which can in principle accommodate more easily the expected changes in metal size upon oxidation/reduction [1]. The Schiff base ligands derived from the reaction of salicylaldehyde with diamines have been extensively studied. These ligands are of great interest mainly due to the existence of (O–H–N and N–H–O) type hydrogen bonds and the possibility of tautomerism [2–5]. Moreover, Schiff base metal complexes containing different metal ions such as Ni, Co, Cu, Mn and Fe have been studied in great details for their various crystallographic features, structure–redox relationships and enzymatic reactions, mesogenic characteristics and catalytic properties [6,7]. Although the magnetic, spectroscopic and catalytic properties of these Schiff-base complexes are well documented [8,9], it still seems that there could be new and specific applications for such a unique class of compound. A considerable number of Schiff-

base complexes have potential biological interest and are used as more or less successful models of biological compounds [10]. Additionally, some of the salicylidene derivatives show photochromism in the solid state [11,12] most likely due to intramolecular proton transfer associated with either a change in π -electron configuration or isomerization in the non-planar molecule [13]. Sterically hindered ligands bearing salicylaldimines are known to be effective antioxidants and are widely used in rancidification of fats and oils [14]. In most steric hindered salicylaldimine, the proton is localized at the oxygen atom and in some cases is attached to the nitrogen atom [15,16]. Proton transfer may occur both in solid and solution states for basic and excited states [15–20]. It has been reported that the transition metal complexes with redox active ligands bearing sterically hindered salicylaldimines undergo one- or two-electron transfer [21]. Redox-active transition metal complexes that stabilize various oxidation states of the metal centers are of considerable interest because of their potential significance as model of redox metalloenzymes [22,23] and as effective redox reactants or catalysts [24]. Furthermore, a recently emerged field of research concerns the use of redox-active metal complexes such as Cu(II) complexes with salen and related Schiff bases as synthetic chemical nucleases or DNA damaging agents [25]. For a specific metal

* Corresponding author. Tel.: +90 4842232082-1230; fax: +90 4842232086.
E-mail address: esreftas@siirt.edu.tr (E. Tas).

ion, the main factors, which are the nature and the arrangement of the donor atoms around the metal bonding site or the nature and the position of substituents, determine redox properties. Among various ligands, many Schiff bases derived from steric hindered salicylaldehyde and related aromatic aldehydes have been found to stabilize copper(I), with the Cu(II/I) redox process [26]. Although the redox behavior of a number of metal complexes containing Schiff base ligands have been known, the electrochemical properties of such complexes are not completely clear [27–30].

In the present study, we report the synthesis and characterization of the new steric hindered ligand (LH₂) involving NONO donor sites and their different mononuclear complexes. It is known that the combination of the electrochemical and spectroelectrochemical methods provides a strong tool to reveal the complementary nature of the molecular structure and electrochemical information of the electroactive molecules [31–40]. The aim of this study is to establish a comparative electro-spectrochemical study on the new Schiff-base mononuclear metal complexes based on the different molecular structures with NONO donor sites. Also, the thermal properties of these metal complexes were investigated in this work.

2. Experimental

2.1. Materials and measurements

All reagents and solvents were of reagent-grade quality and obtained from commercial suppliers (Fluka, Merck and Aldrich). The elemental analyses were carried out in the Laboratory of Inonu University with a Carlo Erba Strumentazione Model 1106 apparatus. IR spectra were recorded on a Perkin Elmer Spectrum RXI FT-IR Spectrometer as KBr pellets. ¹H NMR spectra were recorded on a Bruker-Avance 300 MHz spectrometers. Magnetic susceptibilities were determined on a Sherwood Scientific Magnetic Susceptibility Balance (Model MK1) at room temperature (20 °C) using Hg[Co(SCN)₄] as a calibrant; diamagnetic corrections were calculated from Pascal's constants [41]. Electronic spectral studies were conducted on a Perkin-Elmer model Lambda 25 UV-vis spectrophotometer in the wavelength 200–1100 nm. The thermal analyses measurements (TGA and DTA) were carried out on a Setaram Labsys TG-16 thermobalance under a nitrogen atmosphere. Molar conductivities (Λ_M) were recorded on an Inolab Terminal 740 WTW Series. Cyclic voltammograms (CV) were carried out using CV measurements with Princeton Applied Research Model 2263 potentiostat controlled by an external PC. A three electrode system (BAS model solid cell stand) was used for CV measurements in CH₂Cl₂ and consisted of a 1.6 mm diameter of platinum disc electrode as working electrode, a platinum wire counter electrode, and an Ag/AgCl reference electrode. Tetra-*n*-butylammonium perchlorate (TBAP) was used as a supporting electrolyte. The reference electrode was separated from the bulk solution by a fritted-glass bridge filled with the solvent/supporting electrolyte mixture. The ferrocene/ferrocenium couple (Fc/Fc⁺) was used as an internal standard but all potentials in the paper are referenced to the Ag/AgCl reference electrode. Solutions containing ligand and the metal complexes were deoxygenated by a stream of high purity nitrogen for at least 5 min before running the experiment and the solution was protected from air by a blanket of nitrogen during the experiment. UV-vis spectroelectrochemical experiments were performed with a home-built thin-layer cell that utilized a light transparent platinum gauze working electrode. A platinum wire counter electrode, and Ag/AgCl reference electrode were used for spectroelectrochemical cell. Potentials were applied and monitored with a Princeton Applied Research Model 2263 potentiostat. Time-resolved UV-vis spectra were recorded on Agilent Model 8453 diode array spectrophotometer.

2.2. Synthesis of ligand (LH₂)

The synthesis of the ligand (LH₂) has been reported previously [31]. (Scheme 1). The products are soluble in common solvents such as CHCl₃, C₂H₅OH, DMF and DMSO. ¹H NMR (300 MHz, CDCl₃, Me₄Si, ppm): δ = 13.36 (s, 1H, –OH, D-exchangeable), 13.32 (s, 1H, –OH, D-exchangeable), δ = 8.71 (s, 1H, HC=N), δ = 8.70 (s, 1H, HC=N), δ = 7.88–7.20 (m, 12H, Ar–CH), δ = 1.44–1.43 (d, 18H, J = 3, C–CH₃); δ = 1.33–1.31 (d, 18H, J = 6, C–CH₃). ¹³C NMR (300 MHz, CDCl₃, Me₄Si, ppm): 189.91 (C=O); 160.3, 159.9, 153.2, 153.0 (C=N); 140.9–112.6 (Ar–C); 25.9, 23.8 vs 29.5, 28.5 (C–CH₃).

2.3. General procedure for the synthesis of the metal(II) complexes

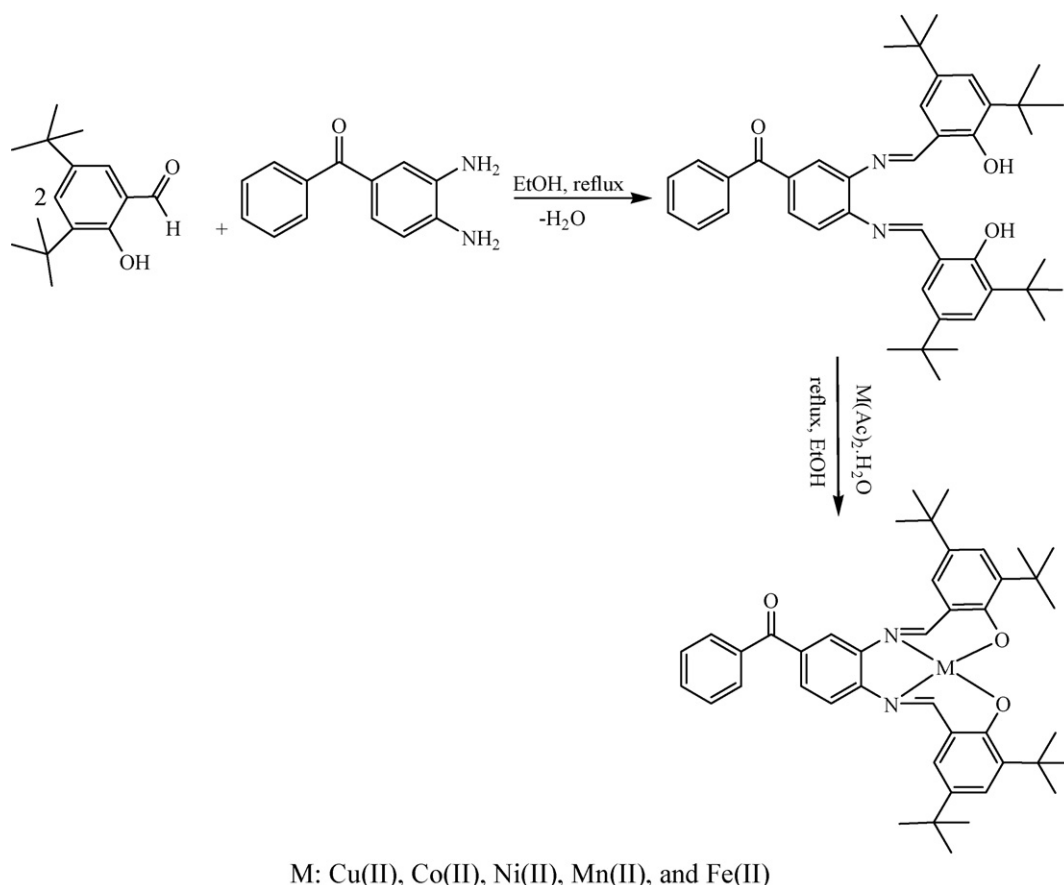
The metal(II) complexes were prepared by the same general method: 10 mmol of the ligand [N,N'-(3,4-benzophenon)-3,5-Bu^t₂-salicylaldehyde (LH₂)] was dissolved in 45 ml absolute ethanol at room temperature (Scheme 1). A solution of 10 mmol of the metal(II) acetate was added dropwise into 20 ml of absolute ethanol under argon atmosphere with continuous stirring. The stirred mixtures were then heated to the reflux temperature and maintained at this temperature for 8–10 h. Then, the mixtures were evaporated to a volume of 10 ml in vacuum and left to cool to the room temperature. The compounds were precipitated after adding 5 ml ethanol. The products were filtered in vacuum and dissolved in chloroform. The chloroform solution was then filtered to separate inorganic salts and the products were precipitated by adding ethanol. And then, they were washed with a small amount of ethanol. The products were recrystallized from ethanol and they were dried at 100 °C. ¹H NMR (300 MHz, DMSO, Me₄Si, ppm): δ = 8.97–8.95 (d, 2H, J = 6, HC=N), δ = 8.32–6.80 (m, 12H, Ar–CH), δ = 1.42–1.10 (m, 36H, C–CH₃) for [Ni(L)] complex.

3. Results and discussion

The ligand [N,N'-(3,4-benzophenon)-3,5-Bu^t₂-salicylaldehyde (LH₂)] (Scheme 1) was obtained from the reaction between 3,5-Bu^t₂-salicylaldehyde and 3,4-diaminobenzophenon in 2:1 molar ratio. The Cu(II), Co(II), Ni(II), Mn(II), and Fe(II) complexes were obtained by a general method using ethanolic solution of metal acetate salt and solution of ligand in absolute ethanol under argon gas (Scheme 1). Three chelate rings were formed by metal(II) coordination to tetradentate steric hindered Schiff bases (with four donor atoms, NONO). The ring formation determines a higher stability of the compounds [42]. The ligand and its metal complexes were formed only in the powder form, which was not suitable for single X-ray diffraction analysis. Further attempts to get crystals were not successful. The ligand (LH₂) on interaction with metal(II) salts yielded complexes corresponding to the general formula [M(L)]. The electrochemical and thin-layer spectroelectrochemical studies of the ligand and its mononuclear metal(II) complexes were comparatively investigated in the same experimental conditions.

3.1. NMR spectra of the ligand and Ni(II) metal complexes

The principal peaks of the ¹H NMR spectra of ligand and its Ni(II) metal complex are given in Section 2. The ¹H NMR spectra of the ligand in the CDCl₃ did not give any signal corresponding to 3,5-Bu^t₂-salicylaldehyde and 3,4-diaminobenzophenon protons. The proton NMR spectra of the free ligand showed two peaks as singlet at 13.36 and 13.32 ppm, which are characteristic of intramolecular hydrogen bonded OH proton. These peaks did not appear in the Ni(II) metal complex as expected. When D₂O was added to the lig-



Scheme 1. Synthetic route of ligand (LH₂) and the suggested mononuclear metal complexes.

and solution, a rapid loss of these signals was observed as expected. The peaks at range 7.88–7.20 ppm for ligand and 8.32–6.80 for Ni(II) metal complex, as multiplet, is assignable to the protons of aromatic –CH groups. In the ¹H NMR spectra of ligand and Ni(II) metal complex, the chemical shifts observed at $\delta = 8.71$ and $\delta = 8.70$ ppm for free ligand as singlet and at $\delta = 8.97$ – 8.95 for Ni(II) metal complex as doublet are assigned to the proton of azomethine (CH=N) [43,44]. However, the protons of the *tert*-butyl groups exhibited two doublet peaks between $\delta = 1.44$ – 1.43 and $\delta = 1.33$ – 1.31 ppm for free ligand and exhibited multiplet peak $\delta = 1.42$ – 1.10 ppm for Ni(II) metal complex. In the ¹³C NMR the imine carbon resonance is found at 160.30, 159.90, 153.20, 153.0 ppm and carbonyl carbon resonance is found at 189.91 ppm for free ligand, respectively. In the spectra of the ¹³C NMR and ¹H NMR of the ligand, the existence of the signals at 160.30 and 159.90 ppm and at 153.20 and 153.00 ppm for carbon double resonances, and at 8.71 and 8.70 ppm for proton double resonances corresponds to the azomethine groups of the molecule, which indicates that the ligand has *cis*–*trans* isomerism [9].

Table 1

The formula, formula weight, colors, melting points, molar conductivity, yields, magnetic susceptibilities and elemental analyses results of the compounds.

Compounds	F.W. (g/mol)	Color	Melting point (°C)	Λ_M ($\Omega^{-1}\text{cm}^2\text{mol}^{-1}$)	Yield (%)	μ_{eff} (B.M.)	Elemental analyses % calculated (found)		
							C	H	N
Ligand (LH ₂) C ₄₃ H ₅₂ N ₂ O ₃	644	Yellow	146	–	75	–	80.09(79.78)	8.13(8.04)	4.34(4.46)
[Cu(L)] C ₄₃ H ₅₀ N ₂ O ₃ Cu	706.4	Dark Green	276	12.6	65	1.74	73.11(72.98)	7.12(6.97)	3.97(3.76)
[Co(L)] C ₄₃ H ₅₀ N ₂ O ₃ Co	701.8	Dark Brown	281	18.3	60	3.35	73.59(72.96)	7.18(6.98)	3.99(3.85)
[Ni(L)] C ₄₃ H ₅₀ N ₂ O ₃ Ni	701.6	Red	286	9.8	70	Dia	73.62(73.27)	7.18(7.17)	3.99(3.82)
[Mn(L)] C ₄₃ H ₅₀ N ₂ O ₃ Mn	697.8	Dark Red	180	13.8	65	3.82	74.01(74.12)	7.22(6.99)	4.01(4.19)
[Fe(L)] C ₄₃ H ₅₀ N ₂ O ₃ Fe	698.7	Black	150	11.7	70	3.90	73.92(74.41)	7.21(7.10)	4.01(3.95)

Table 2

Characteristic IR bands (cm⁻¹) of the ligand and its complexes as KBr pellets.

Compounds	$\nu(\text{OH}\cdots\text{N})$	$\nu(\text{Aliph C-H})$	$\nu(\text{C=O})$	$\nu(\text{C=N})$	$\nu(\text{C-O})$
Ligand (LH ₂)	2219–3505	2869–2965	1657	1615	1172
[Cu(L)]	–	2839–2985	1643	1602	1171
[Co(L)]	–	2850–2980	1645	1610	1175
[Ni(L)]	–	2847–2978	1648	1608	1178
[Mn(L)]	–	2868–2956	1647	1599	1177
[Fe(L)]	–	2850–2960	1651	1598	1177

3.2. FT-IR spectra of the ligand and its metal(II) complexes

The main IR characteristic stretching frequencies of the ligand and its metal complexes along with their proposed assignments are summarized in Table 2. The IR spectra of the metal complexes are similar to each other, except for some slight shifts and intensity changes of a few vibration peaks caused by different metal(II) ions, which indicates that the metal complexes have similar structure. However, there are some significant differences between the

metal(II) complexes and its free ligand upon chelation, as expected. The coordination mode and sites of ligand to the metal ions were investigated by comparing the IR spectra of the free ligand with its metal complexes. Upon coordination, it is noteworthy that the peak at 1657 cm^{-1} for ligand attributed to $\nu(\text{C}=\text{O})$ vibration was shifted to a lower wavenumber [45]. The coordination of the steric hindered ligand with the different metals through the nitrogen atom is expected to reduce the electron density in the azomethine link and lower the $\nu(\text{C}=\text{N})$ absorption frequency. The very strong and sharp bands located at 1615 cm^{-1} are assigned to the $\nu(\text{C}=\text{N})$ stretching vibrations of the azomethine of the ligand. These bands are shifted by $17\text{--}5\text{ cm}^{-1}$ to lower wavenumber. These shifts support the participation of the azomethine group of this ligand in binding to the Cu(II), Co(II), Ni(II), Mn(II), and Fe(II) ions [11,46,47]. In addition, the IR spectrum of the ligand revealed a sharp peak at 1172 cm^{-1} belonging to phenolic C–O stretching which is slightly shifted to lower or higher frequency range $1171\text{--}1178\text{ cm}^{-1}$ after complexation in all metal complexes, suggesting that the phenolic oxygen participates in the coordination mode. This has been further supported by the disappearance of the broad $\nu(\text{OH}\cdots\text{N})$ peak around $2219\text{--}3505\text{ cm}^{-1}$ in the all metal complexes, indicating deprotonation of the phenolic proton prior to coordination [48].

3.3. UV–vis spectra of the ligand and its metal complexes

Electronic spectra of ligand and its mononuclear Cu(II), Co(II), Ni(II), Mn(II), and Fe(II) complexes have been recorded in the $200\text{--}1100\text{ nm}$ range in CHCl_3 , DMSO and EtOH solutions and their corresponding data are given in Table 3. The formation of the metal complexes was also confirmed by electronic spectra. In the electronic spectra of the ligand and its mononuclear metal complexes, the wide range bands were observed due to either the $\pi \rightarrow \pi^*$ and $n \rightarrow \pi^*$ of C=N chromophore or charge-transfer transition arising from π electron interactions between the metal and ligand, which involves either a metal-to-ligand or ligand-to-metal electron transfer [49–52]. The electronic spectra of the free ligands in CHCl_3 and DMSO showed strong absorption bands in the ultraviolet region ($263\text{--}408\text{ nm}$), that could be attributed respectively to the $\pi \rightarrow \pi^*$ and $n \rightarrow \pi^*$ transitions in the benzene ring or azomethine ($-\text{C}=\text{N}$) groups for free ligand. In the electronic spectra of the metal complexes, the band of the high or low wavelength side shows an inequable bathochromic or hypsochromic shifts relative to its free ligand in different solutions. The absorption bands between 263 and 408 nm in free ligand change a bit in intensity and remain essentially slightly changed for metal complexes. The absorption

shift and intensity change in the spectra of the metal complexes most likely originate from the metalation which increases the conjugation and delocalization of the whole electronic system and results in the energy change of the $\pi \rightarrow \pi^*$ and $n \rightarrow \pi^*$ transition of the conjugated chromophore [53,54]. The results clearly indicate that the ligand coordinates to Cu(II), Co(II), Ni(II), Mn(II), and Fe(II) ions, which are in accordance with the results of the other spectral data. Furthermore, in the case of the Cu(II), Co(II), Ni(II), Mn(II), and Fe(II) complexes, the absorption bands in the visible region are observed at between 460 and 634 nm for Cu(II) complex, at between 452 and 510 nm for Co(II) complex, at between 503 and 559 nm for Ni(II) complex, at between 494 and 513 nm for Mn(II) complex and at between 434 and 619 nm for Fe(II) complex (in CHCl_3 , DMSO and EtOH) as a low intensity bands. These bands are considered to arise from the forbidden d–d transition, which is generally too weak. The nature of the Cu(II), Co(II), Ni(II), Mn(II), and Fe(II) ions affects the position of absorption band significantly [55]. According to modern molecular orbital theory [56], any factors that can influence the electronic density of conjugated system must result in the bathochromic or hypsochromic shift of absorption bands. Here, in the case of the metal complexes with same ligand, the main reason of bathochromic or hypsochromic shifts is generally related with the electronegativity of the different metal ions [53].

3.4. Magnetic moments of metal complexes

Magnetic susceptibility measurements provide sufficient data to characterize the structure of the metal complexes. Magnetic moments measurements of compounds were carried out at 25°C . The room temperature magnetic moment of Cu(II) metal complex was found at 1.74 B.M. which was typical for mononuclear of Cu(II) compounds with a $S = 1/2$ spin state and did not indicate antiferromagnetic coupling of spin at this temperature. These results are comparable to the values reported for slightly distorted tetrahedral geometry [20,57]. The room temperature magnetic moment of the Co(II) complex was found at 3.55 B.M. which was close to the spin-only magnetic moments ($\mu = 3.87\text{ B.M.}$) for three unpaired electrons. Diamagnetic nature of the Ni(II) complex was also confirmed by the magnetic susceptibility measurement. The room temperature magnetic moment of the Mn(II) complex was found at 3.82 B.M. and found at 3.90 B.M. for the Fe(II) complex (Table 1).

3.5. Molar conductivity

With a view to studying the electrolytic nature of the mononuclear metal complexes, their molar conductivities were measured in DMF (dimethyl formamide) at 10^{-3} M . The molar conductivities (Λ_M) values of these metal complexes are in the range of $9.8\text{--}18.3\ \Omega^{-1}\text{cm}^2\text{ mol}^{-1}$ at room temperature, indicating their almost non-electrolytic nature (Table 1). These low values indicates that mononuclear metal complexes are non-electrolytes due to lack of counter ions in the proposed structures of the mononuclear metal complexes (Scheme 1) [58]. The difference in the number of protons in the mononuclear Cu(II), Co(II), Ni(II), Mn(II) and Fe(II) metal complexes probably points the difference in the sizes of the +2 oxidation state of these metal ions, with the different polarizing due to its different sizes.

3.6. Thermal properties of the ligand and its metal complexes

The thermal properties of the ligand and its metal complexes were investigated by thermal gravimetric analysis (TGA) and thermal differential analysis (DTA). Fig. 1 shows the recorded TGA and DTA curves of ligand (a) and its Ni(II) and Mn(II) (b and c) metal complexes under a nitrogen atmosphere. The samples were heated up at 1 atm pressure with a heating rate of $10^\circ\text{C min}^{-1}$ and a tem-

Table 3
UV–vis data of the ligand and its metal complexes.

Compounds	Solvent	Wavelength [λ_{max} /(nm)]				
Ligand (LH ₂)	CHCl_3	284	301	408		
	DMSO	263	339			
[Cu(L)]	CHCl_3	254	327	350	460	
	DMSO	260	324	452	634	
	$\text{C}_2\text{H}_5\text{OH}$	264	322	426	530	
[Co(L)]	CHCl_3	258	332	358	452	
	DMSO	266	318	423	510	
	$\text{C}_2\text{H}_5\text{OH}$	253	280	332	344	453
[Ni(L)]	CHCl_3	267	305	396	519	559 ^a
	DMSO	270	303	390	503	
	$\text{C}_2\text{H}_5\text{OH}$	265	302	392	505	
[Mn(L)]	CHCl_3	255	305	366 ^a	494	
	DMSO	260	320	357	479	
[Fe(L)]	CHCl_3	240	313	434		
	DMSO	260	314	400	459	619 ^a

^a Shoulder peak.

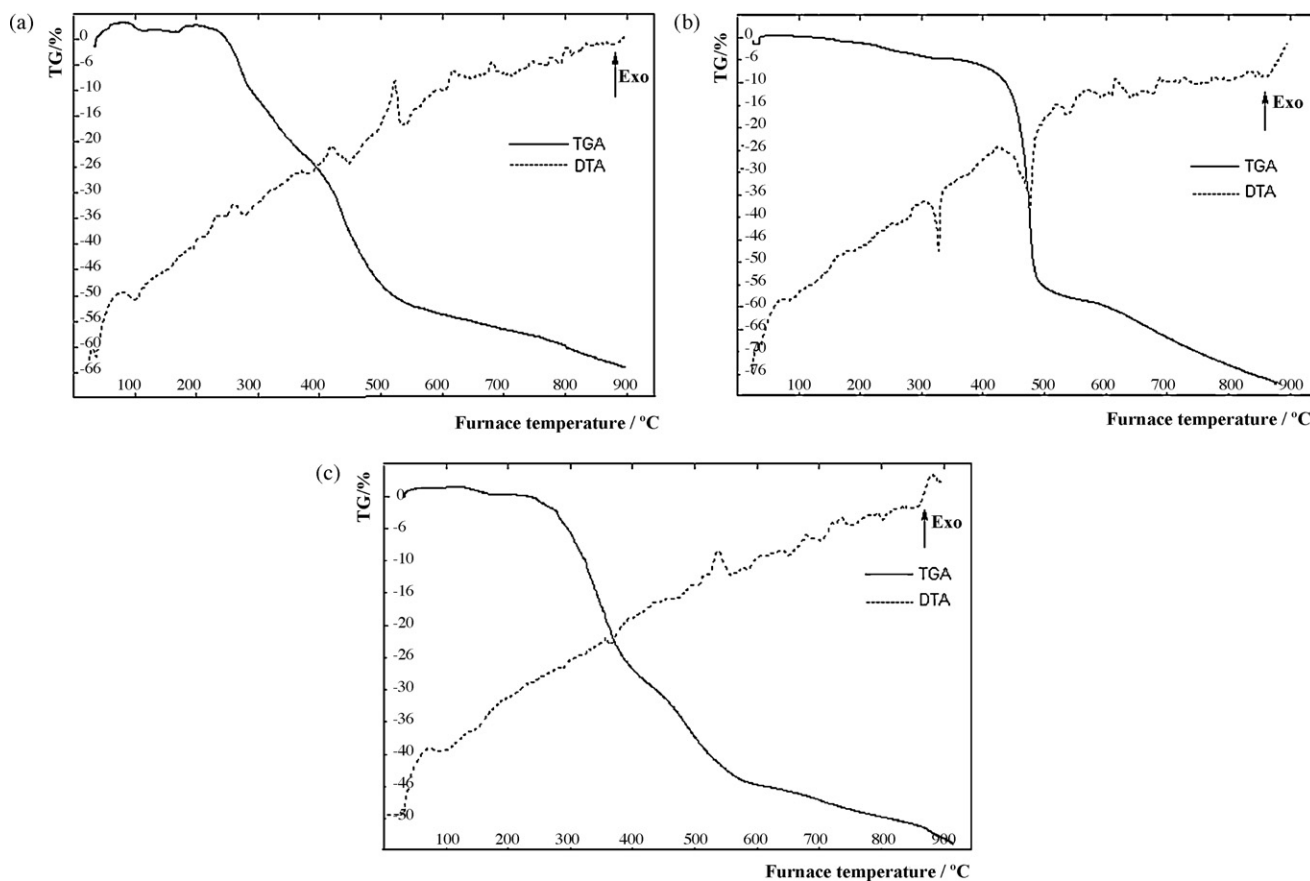


Fig. 1. The TGA and DTA curves of (a) ligand (LH₂), (b) [Ni(L)] and (c) [Mn(L)] metal complexes.

perature range of 20–900 °C. The thermal decomposition of ligand and its metal complexes are seen to be irreversible. It can be seen that TGA curve of the ligand (Fig. 1a) and its Ni(II) and Mn(II) (b and c) metal complexes shows no mass loss up to 182 °C, indicating the absence of water molecules and any other adsorptive solvents molecules in coordination sphere. As the temperature is increased, the thermal decomposition of the ligand occurs at three steps (Fig. 1a). The first degradation step takes place in the range of 212–395 °C which is a weight loss 30.9% and associated with exothermic peaks at 240 and 261 °C with endothermic peak at 276 °C. For ligand, the second degradation step takes place in the range of 424–533 °C which is a weight loss 61.4% and associated with exothermic peaks at 420 and 522 °C with endothermic peak at 447 °C. The third degradation step takes place in the range of 579–900 °C which is a weight loss 64.4% and associated with two exothermic peaks at 619 and 679 °C. The TGA curves of the metal complexes give two or three-stage decomposition pattern within the ranges 20–900 °C. The first degradation step takes place in the range of 287–419 °C which is a weight loss 36.6% and associated with exothermic peaks at 263 and 374 °C with endothermic peak at 290 and 391 °C. The second degradation step takes place in the range of 441–867 °C which is a weight loss 60.1% and associated with exothermic peaks at 646 and 735 °C with endothermic peak at 497 °C for Cu(II) metal complexes. For Co(II) metal complex, the first degradation step takes place in the range of 184–393 °C which is a weight loss 42.7% and associated with endothermic peak at 346 and 382 °C, the second degradation step takes place in the range of 465–900 °C which is a weight loss 68% and associated with exothermic peaks at 533, 751 and 783 °C with endothermic peak at 597 and 819 °C. For Ni(II) metal complex, the first degradation

step takes place in the range of 211–316 °C which is a weight loss 4.1% and associated with endothermic peak at 327 °C, the second degradation step takes place in the range of 389–494 °C which is a weight loss 54% and associated with exothermic peaks at 538 °C with endothermic peak at 473 °C, the third degradation step takes place in the range of 590–900 °C which is a weight loss 77.6% and associated with exothermic peaks at 617 °C with endothermic peak at 643 and 679 °C (Fig. 1b). For Fe(II) metal complex, the first degradation step takes place in the range of 182–416 °C which is a weight loss 45.8% and associated with exothermic peaks at 574 °C with endothermic peak at 349 and 379 °C, the second degradation step takes place in the range of 467–900 °C which is a weight loss 68.1% and associated with exothermic peaks at 532, 753 and 784 °C with endothermic peak at 602 and 818 °C. For Mn(II) metal complex, the first degradation step takes place in the range of 247–398 °C which is a weight loss 27.4% and associated with endothermic peak at 363 °C, the second degradation step takes place in the range of 447–586 °C which is a weight loss of 45.2% and associated with exothermic peaks at 536 °C with endothermic peak at 560 °C, the third degradation step takes place in the range of 657–900 °C which is a weight loss 55.0% and associated with exothermic peaks at 684 and 740 °C with endothermic peak at 706 and 754 °C (Fig. 1c), respectively [59]. As we look at the beginning to decompose temperature, data also reveal that the most stable compound is Cu(II) metal complex while the least stable compound is Fe(II) metal complex. Hence Cu(II) is metal complex decompose later. [60]. From the TGA and DTA results, mononuclear metal complexes have different thermal stabilities, which may be attributed to the fact that the M–N and M–O bonds are different highly polarized [61].

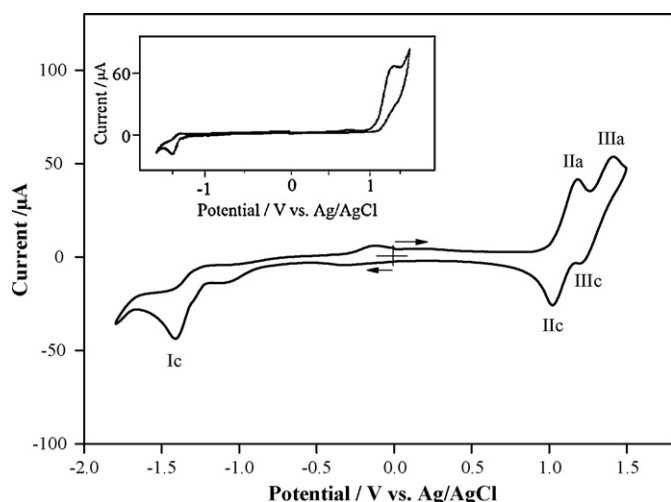


Fig. 2. Cyclic voltammogram (CV) of [Ni(L)] in CH_2Cl_2 containing 0.1 M TBAP. Scan rate: 0.010 V s^{-1} . Working electrode: a 1.6 mm diameter of platinum disc electrode. $c = 4.0 \times 10^{-3} \text{ M}$. The inset figure presents the CV of the ligand (LH_2) in the same experimental conditions.

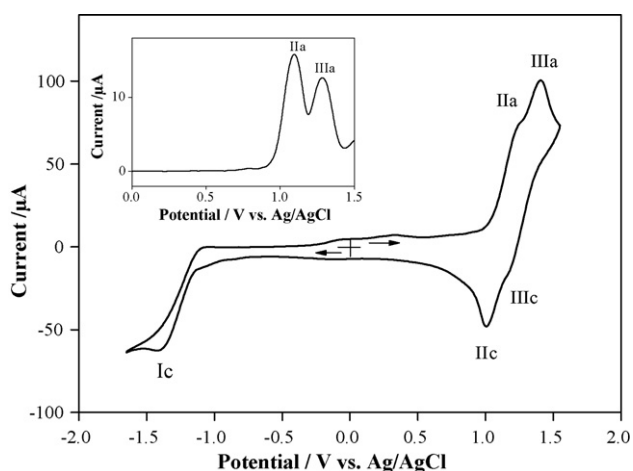


Fig. 3. Cyclic voltammogram (CV) of [Cu(L)] in CH_2Cl_2 containing 0.1 M TBAP. Scan rate: 0.010 V s^{-1} . Working electrode: a 1.6 mm diameter of platinum disc electrode. $c = 4.0 \times 10^{-3} \text{ M}$. The inset figure presents the DPV of the complex in the same experimental conditions.

3.7. Electrochemistry and spectroelectrochemistry

Electrochemistry of the ligand (LH_2) and its metal complexes, [Ni(L)], [Cu(L)], and [Mn(L)], were studied by cyclic voltammetry in scan rate of 0.010 V s^{-1} in dichloromethane (CH_2Cl_2) solution containing 0.1 M TBAP supporting electrolyte. Cyclic voltammograms (CVs) of the ligand and complexes are given in Figs. 2–4 and their voltammetric data are listed in Table 4. Fig. 2 repre-

Table 4
Voltammetric data for the ligands and their copper complexes versus Ag/AgCl in CH_2Cl_2 -TBAP.

Compounds	(L)/(L) ^{-a}	(L)/(L) ^{+b}	M(II)/M(I) ^a	M(II)/M(III) ^c
Ligand (LH_2)	-1.45	1.20 ^a		
[Ni(L)]	-1.41	1.10 ^c (0.12)		1.32 (0.17)
[Cu(L)]	-1.39	1.11 ^c (0.18)		1.30 (0.20)
[Mn(L)]	-1.66	1.25 ^d	-0.62	1.43 (0.19)

^a E_{pc} : cathodic peak potential for reduction for irreversible processes.

^b $\Delta E_p = E_{\text{pc}} - E_{\text{pa}}$ at 0.010 V s^{-1} scan rate (the values given in parentheses).

^c $E_{1/2} = E_{\text{pc}} + E_{\text{pa}}/2$.

^d E_{pa} : anodic peak potential for oxidation for irreversible processes.

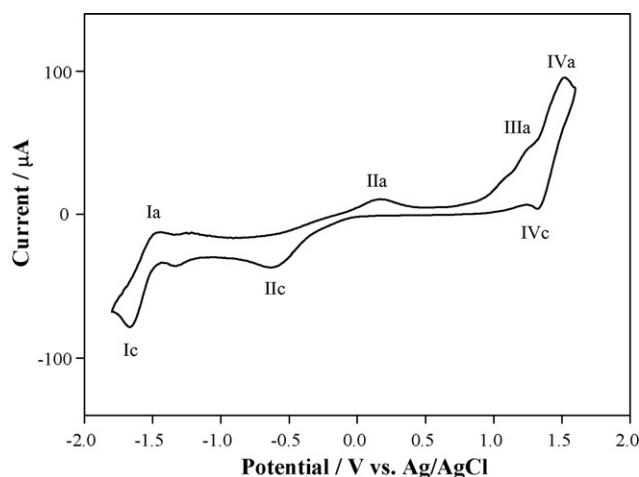


Fig. 4. Cyclic voltammogram (CV) of [Mn(L)] in CH_2Cl_2 containing 0.1 M TBAP. Scan rate: 0.010 V s^{-1} . Working electrode: a 1.6 mm diameter of platinum disc electrode. $c = 4.0 \times 10^{-3} \text{ M}$.

sents the CV of the nickel complex [Ni(L)] where the CV of the ligand is also given as a inset figure. The ligand showed one irreversible oxidation at 1.20 V (E_{pa}) and one irreversible reduction at -1.45 V (E_{pc}) versus Ag/AgCl in the scan rate of 0.010 V s^{-1} . [Ni(L)] exhibited two anodic waves (IIa and IIIa) with corresponding cathodic waves (IIc and IIIc) and one cathodic wave (Ic) without corresponding anodic wave. The anodic wave (IIa) belonging to the first oxidation is assigned to ligand-based oxidation. The cathodic peak waves of the first oxidation and reduction processes of the complex [Ni(L)] appeared almost at the same position with those of the ligand, indicating that the first oxidation and reduction processes of the complex is based on the ligand. The first and second oxidation processes of [Ni(L)] are quasi-reversible with the corresponding anodic-cathodic peak separations (ΔE) for the (L)/(L)⁺ couples (0.12 V at scan rate 0.010 V s^{-1}) and Ni(II)/Ni(III) couples (0.17 V at scan rate 0.010 V s^{-1}). Half-wave potentials ($E_{1/2}$) of (L)/(L)⁺ and Ni(II)/Ni(III) couples were calculated as the average of the anodic and cathodic peak potentials of the processes, which are given in Table 4. Fig. 3 represents the CV of the copper complex [Cu(L)] where the inset figure exhibits differential pulse voltammogram (DPV) of the complex. [Cu(L)] showed two quasi-reversible oxidation and one irreversible reduction processes. This electrochemical behavior is similar to that of the [Ni(L)] in the same experimental conditions. The combined anodic waves (IIa and IIIa) observed for the CV of [Cu(L)] could be separated by differential pulse voltammetry. No considerable difference was observed for the voltammetric data of [Cu(L)] compared with those of the [Ni(L)]. Fig. 4 presents the CV of the manganese complex [Mn(L)] which exhibits considerably different electrochemical behavior compared with [Ni(L)] and [Cu(L)] complexes. [Mn(L)] gave two oxidation and two reduction processes. The first and second oxidation processes are based on the ligand and metal center, respectively as observed for the [Ni(L)] and [Cu(L)] complexes. The first oxidation which has no corresponding cathodic wave is irreversible while the second oxidation with a corresponding anodic wave is quasi-reversible. The cathodic wave (IIc) belongs to a reduction of metal center Mn(II)/Mn(I). This reduction process has irreversible character with the large anodic-cathodic peak separation (ΔE) for the Mn(II)/Mn(I) couples (0.455 V at scan rate 0.010 V s^{-1}), probably due to a low electron transfer on the electrode surface. The second reduction process is based on the ligand as observed for [Ni(L)] and [Cu(L)] complexes. The half-wave potential of the oxidation process based on the Mn(II)/Mn(III) couples shifted toward more positive value while the cathodic peak potential (E_{pc}) of the reduction pro-

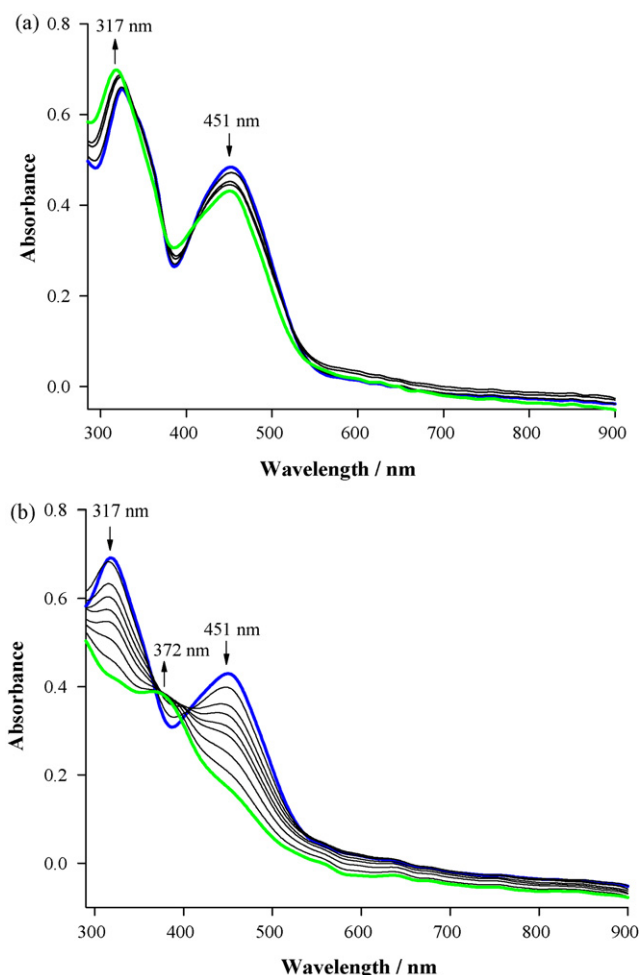


Fig. 5. Time-resolved UV-vis spectra of [Cu(L)] in CH_2Cl_2 containing 0.4 M TBAP (a) during the first oxidation at $E_{\text{app}} = 1.30 \text{ V}$ and (b) during the second oxidation at $E_{\text{app}} = 1.60 \text{ V}$.

cess based on the ligand $(\text{L})/(\text{L})^-$ negatively shifted compared with those of $[\text{Ni}(\text{L})]$ and $[\text{Cu}(\text{L})]$.

The spectroelectrochemical behaviors of the ligand (LH_2) and its metal complexes were investigated using a thin-layer UV-vis spectroelectrochemical technique in CH_2Cl_2 solution containing 0.4 M TBAP. The UV-vis spectral changes for the reduced and oxidized species were obtained in a thin-layer cell during applied potentials. The absorption spectra of electrochemically generated species are given in Figs. 5–7. The convenient values of applied potentials for *in situ* spectroelectrochemical experiment were determined for the reduction and oxidation processes by taking CVs of the metal complex in the thin-layer cell.

Fig. 5a shows changes in the electronic spectra of $[\text{Cu}(\text{L})]$ during the first oxidation process in the thin-layer cell. When the potential ($E_{\text{app}} = 1.30 \text{ V}$) was applied in the thin layer cell, intensity of the main band at 451 nm belonging to the $n \rightarrow \pi^*$ transitions of the azomethine ($\text{CH}=\text{N}$) decreased. The similar behavior was observed for the ligand in the same experimental conditions but where isosbestic points could not clearly seen probably due to a fast chemical decomposition or a chemical coupling of the electro-generated oxidized species in the time scale of spectroelectrochemical measurements. These results confirm the ligand-based first oxidation process of the complex. Fig. 5b exhibits changes in the electronic spectra of $[\text{Cu}(\text{L})]$ during the second oxidation process (the applied potential ($E_{\text{app}} = 1.60 \text{ V}$)). As seen, two main bands at 451 and 317 nm disappeared and a new band formed at 372 nm dur-

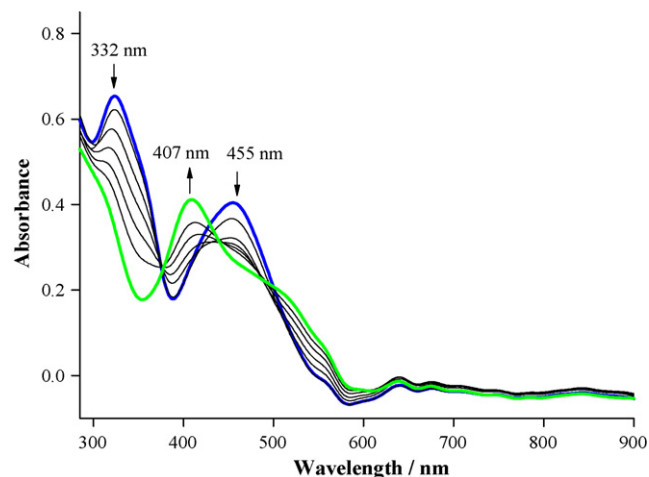


Fig. 6. Time-resolved UV-vis spectra of $[\text{Cu}(\text{L})]$ during the reduction at $E_{\text{app}} = -1.65 \text{ V}$.

ing the oxidation process. The original spectrum of the neutral complex could be recovered when the potential was applied at $E_{\text{app}} = 0.40 \text{ V}$ for the re-reduction process, indicating that the doubly electro-reduced products remain stable in the thin layer cell throughout the experiment. Fig. 6 shows changes in the electronic spectra of $[\text{Cu}(\text{L})]$ during the reduction process in the thin-layer cell ($E_{\text{app}} = -1.65 \text{ V}$). The main bands at 455 and 332 nm disappeared

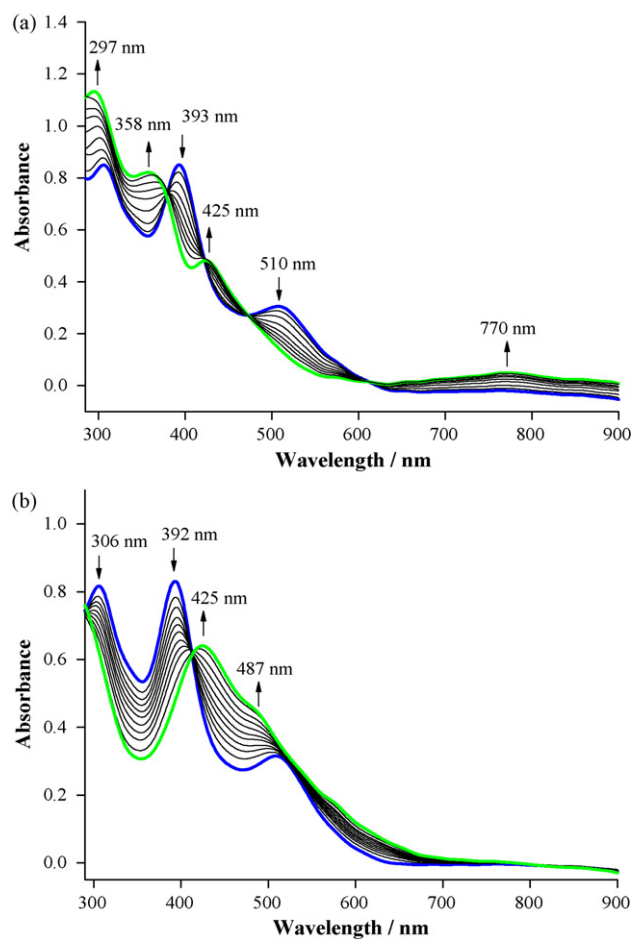


Fig. 7. Time-resolved UV-vis spectra of $[\text{Ni}(\text{L})]$ in CH_2Cl_2 containing 0.4 M TBAP (a) during the second oxidation at $E_{\text{app}} = 1.60 \text{ V}$ and (b) during the reduction at $E_{\text{app}} = -1.65 \text{ V}$.

and a new band evolved at 407 nm during the reduction process. The original spectrum corresponding to the neutral complex could not be recovered when the potential was applied at $E_{app} = -0.60$ V for the re-oxidation process which indicates that the reduced species is not stable during the process. Fig. 7a shows changes in the electronic spectra of [Ni(L)] during the second oxidation process in the thin-layer cell ($E_{app} = 1.60$ V). The well-defined isosbestic points were observed at 377, 420, 472, and 609 nm, confirming that the electrode reaction proceeds in a quantitative fashion and therefore the absence of any coupled chemistry [9,31,36–38]. During the oxidation process, the bands at 393 and 510 nm disappeared and a new bands formed at 358, 425, and 770 nm. It was also seen that intensity of band at 297 nm increased. The main band at 393 nm belonging to the $n \rightarrow \pi^*$ transitions of the azomethine (CH=N) shifted to a shorter wavelength. This spectral changes is similar to what is observed for [Ni(L)]. Fig. 7b presents changes in the electronic spectra of [Ni(L)] during the reduction process in the thin-layer cell ($E_{app} = -1.65$ V). The main band at 425 nm disappeared and a new band formed at 392 nm in addition to an increase in intensity of the band at 306 nm. Appearance of the final spectrum of electro-reduced species of [Ni(L)] is similar to that of [Cu(L)], which assigns to ligand-based reduction process.

4. Conclusion

New steric hindered ligand (LH₂), [N, N'-(3,4-benzophenon)-3,5-Bu^t₂-salicylaldehyde (LH₂)] and its mononuclear Cu(II), Co(II), Ni(II), Mn(II), and Fe(II) complexes were synthesized and their electro-spectrochemical properties were investigated using the cyclic voltammetric and thin-layer spectroelectrochemical techniques in CH₂Cl₂. Besides the classical methods such as FT-IR, UV-vis, ¹H NMR spectra, elemental analysis, magnetic susceptibility, thermal properties and molar conductivity for structural characterization, the combination of the electrochemical and spectroelectrochemical methods provided a power tool to reveal the complementary nature of the molecular structure and electron-transfer reactions of the reduced species of new electroactive steric hindered Schiff-bases and its mononuclear Cu(II), Ni(II), Mn(II) complexes. As we look at the begins to decompose temperature, data also reveal that the most stable compound is Cu(II) complex while the least stable compound is Fe(II) complex. The molar conductivities (Λ_M) values of these metal complexes are in the range of 9.8–18.3 $\Omega^{-1}\text{cm}^2\text{mol}^{-1}$ at room temperature, indicating their almost non-electrolytic nature. The analytical results agree with the expected structure and other data are given in Section 2 and Scheme 1.

Acknowledgements

This work have been supported, in part, by the Technological and Scientific Research Council of Turkey TUBITAK (TBAG Project No.: 106T085) and by the Harran University Research Fund (HUBAK, Grant No.: 752) is gratefully acknowledged.

References

- [1] B.S. Garg, D.N. Kumar, Spectrochim. Acta A 59 (2) (2003) 229.
- [2] F. Cristina, B. de Castro, J. Chem. Soc., Dalton Trans. (1998) 1491.
- [3] K.B. Gudasi, M.S. Patil, R.S. Vadavi, R.V. Shenoy, S.A. Patil, Trans. Met. Chem. 31 (2006) 986.
- [4] M. Odabasoglu, C. Albayrak, R. Ozkanca, F.Z. Akyan, P. Lönnecke, J. Mol. Struct. (2007) 840–889.
- [5] A. Ozek, C. Albayrak, M. Odabasoglu, O. Büyükgüngör, Acta Cryst. C63 (2007) 177.
- [6] A.J. Stemmler, C.J. Burrows, J. Am. Chem. Soc. 121 (29) (1999) 6956.
- [7] R. Klement, F. Stock, H. Elias, H. Paulus, P. Pelikan, M. Valko, M. Mazur, Polyhedron 18 (27) (1999) 3617.
- [8] N. Re, E. Gallo, C. Floriani, H. Miyasaka, N. Matsumoto, Inorg. Chem. 35 (21) (1996) 5964.
- [9] A. Kilic, E. Tas, B. Deveci, I. Yilmaz, Polyhedron 26 (2007) 4009.
- [10] K.S. Suslick, T.J. Reinert, J. Chem. Educ. 62 (11) (1988) 974.
- [11] L. Mishra, K. Bindu, S. Bhattacharya, Inorg. Chem. Commun. 7 (6) (2004) 777.
- [12] M.D. Cohen, G.M.J. Schmidt, J. Phys. Chem. 66 (1962) 2442.
- [13] P.F. Barbara, P.M. Rentzepis, L.E. Brus, J. Am. Chem. Soc. 102 (8) (1980) 2786.
- [14] D. Zurita, I. GautierLuneau, S. Menage, J.L. Pierre, E. SaintAman, J. Biol. Inorg. Chem. 2 (1) (1997) 46.
- [15] T. Inabe, I. Luneau, T. Mitani, Y. Maruyama, S. Takeda, Bull. Chem. Soc. Jpn. 67 (3) (1994) 612.
- [16] H. Naeimi, K. Rabiei, F. Salimi, Dyes Pigm. 75 (2007) 294.
- [17] E. Hadjoudis, M. Vittorakis, I. Moustakalimavridis, Tetrahedron 43 (7) (1987) 1345.
- [18] T. Sekikawa, T. Kobayashi, T. Inabe, J. Phys. Chem. 101 (4) (1997) 644.
- [19] M.L. Glowka, D. Martynowski, K. Kozłowska, J. Mol. Struct. 474 (1999) 81.
- [20] E. Tas, A. Kilic, N. Konak, I. Yilmaz, Polyhedron 27 (3) (2008) 1024.
- [21] J.F. Larrow, E.N. Jacobsen, Y. Gao, Y.P. Hong, X.Y. Nie, C.M. Zepp, J. Org. Chem. 59 (7) (1994) 1939.
- [22] R.H. Holm, P. Kennepohl, E.I. Solomon, Chem. Rev. 96 (7) (1996) 2239.
- [23] M. Vaidyanathan, R. Viswanathan, M. Palaniandavar, T. Balasubramanian, P. Prabhakaran, T.P. Muthiah, Inorg. Chem. 37 (25) (1998) 6418.
- [24] W. Adam, R.T. Fell, V.R. Stegmann, C.R. Saha-Möller, J. Am. Chem. Soc. 120 (1998) 708.
- [25] C.J. Burrows, J.G. Muller, Chem. Rev. 98 (1998) 1109.
- [26] J. Costamagana, J. Vargas, R. Latorre, A. Alvarado, G. Mena, Coord. Chem. Rev. 119 (1992) 67.
- [27] E. Tas, M. Aslanoglu, A. Kilic, O. Kaplan, H. Temel, J. Chem. Res.-(S) 4 (2006) 242.
- [28] E. Tas, I. Ucar, V.T. Kasumov, A. Kilic, A. Bulut, Spectrochim. Acta A 68 (2007) 463.
- [29] G. Karthikeyan, P. Pitchaimani, Trans. Met. Chem. 28 (4) (2003) 482.
- [30] S. Ilhan, H. Temel, I. Yilmaz, A. Kilic, Trans. Met. Chem. 32 (3) (2007) 344.
- [31] E. Tas, A. Kilic, M. Durgun, I. Yilmaz, I. Ozdemir, N. Gurbuz, J. Organomet. Chem. 694 (3) (2009) 446.
- [32] I. Yilmaz, A.G. Gurek, V. Ahsen, Polyhedron 24 (7) (2005) 791.
- [33] I. Yilmaz, M. Kocak, Polyhedron 23 (7) (2004) 1279.
- [34] K.M. Kadish, T. Nakanishi, A.G. Gürek, V. Ahsen, I. Yilmaz, J. Phys. Chem. B 105 (2001) 9817.
- [35] I. Yilmaz, T. Nakanishi, A. Gürek, K.M. Kadish, J. Porhy. Phthal. 7 (2003) 227.
- [36] T. Nakanishi, I. Yilmaz, N. Nakashima, K.M. Kadish, J. Phys. Chem. B 107 (2003) 12789.
- [37] S. Arslan, I. Yilmaz, Polyhedron 26 (2007) 2387.
- [38] S. Arslan, I. Yilmaz, Trans. Met. Chem. 32 (2007) 292.
- [39] S. Arslan, I. Yilmaz, Inorg. Chem. Commun. 10 (2007) 385.
- [40] J. Losada, I. del Peso, L. Beyer, Inorg. Chim. Acta 321 (1,2) (2001) 107.
- [41] A. Earnshaw, Introduction to Magnetochemistry, Academic Press, London, 1968, p. 4.
- [42] A. Pui, C. Polcar, J.P. Mahy, Inorg. Chim. Acta 360 (6) (2007) 2139.
- [43] H. Khanmohammadi, M. Darvishpour, Dyes Pigm. 81 (3) (2009) 167.
- [44] S. Ilhan, H. Temel, A. Kilic, J. Coord. Chem. 61 (2) (2008) 277.
- [45] Z. Chen, Y. Wu, D. Gu, F. Gan, Dyes Pigm. 76 (3) (2008) 624.
- [46] H. Temel, S. Ilhan, A. Kilic, E. Tas, J. Coord. Chem. 61 (9) (2008) 1443.
- [47] A. Vogt, S. Wolowicz, R.L. Prasas, A. Gupta, J. Skarzewski, Polyhedron 17 (8) (1998) 1231.
- [48] K.N. Kumar, R. Ramesh, Polyhedron 24 (14) (2005) 1885.
- [49] L. Sacconi, M. Ciampolini, F. Maffio, F.P. Cavasino, J. Am. Chem. Soc. 84 (1962) 3246.
- [50] R.L. Carlin, Trans. Met. Chem., vol. 1, Marcel Dekker, New York, 1965, p. 239.
- [51] E. Tas, M. Aslanoglu, A. Kilic, Z. Kara, J. Coord. Chem. 59 (8) (2006) 861.
- [52] M. Odabasoglu, F. Arslan, H. Olmez, O. Buyukgungor, Dyes Pigm. 75 (3) (2007) 507.
- [53] Z. Chen, Y. Wu, D. Gu, F. Gan, Spectrochim. Acta A 68 (3) (2007) 918.
- [54] Z. Chen, F. Huang, Y. Wu, D. Gu, F. Gan, Inorg. Chem. Commun. 9 (1) (2006) 21.
- [55] C.C. Leznoff, A.B.P. Lever (Eds.), Phthalocyanines, Properties and Applications, 1 ed., vols. 1–4, VCH Publishers, Wiley-VCH, New York, Weinheim, Cambridge, 1996, p. 524.
- [56] V.T. Kasumov, Spectrochim. Acta A 57 (8) (2003) 1649.
- [57] W.J. Geary, Chem. Rev. 7 (1) (1971) 81.
- [58] A. Kilic, E. Tas, Synt. React. Inorg. Met. -Org. Nano-Met. Chem. 37 (8) (2007) 583.
- [59] V.T. Yilmaz, S. Hamamci, O. Buyukgungor, Polyhedron 27 (6) (2008) 1761.
- [60] K. Nejadi, Z. Rezvani, B. Massoumi, Dyes Pigm. 75 (2007) 653.
- [61] O.G. Wu, M. Esteghamatian, N.X. Hu, Z. Popovic, G. Enright, S. Wang, Y. Tao, M. D'lorio, Chem. Mater. 20 (2000) 79.